Sensors and Materials, Vol. 34, No. 7 (2022) 2747–2758
MYU Tokyo

S & M 3003

Portable Skin-injury Monitoring Device for Early Diagnosis of Pressure Ulcers

Lan Zhang,[1*] En Takashi,[2] Jian Lu,[1] Akio Kamijo,[2] and Akio Kitayama[2]

[1]Device Technology Research Institute, National Institute of Advanced Industrial Science and Technology (AIST), 1-2-1 Namiki, Tsukuba, Ibaraki 305-8564, Japan
[2]Faculty of Nursing, Nagano College of Nursing, 1694 Akaho, Komagane, Nagano 399-4117, Japan

(Received August 26, 2021; accepted November 24, 2021)

Keywords: skin injury, early diagnosis, pressure ulcer, load cell, LED

Pressure ulcers are a skin condition caused by friction, shear, and long-term pressure on the skin and can result in considerable discomfort for patients. We developed a novel monitoring device for the early diagnosis of pressure ulcers. We designed and fabricated the diagnosis, transmission, and recording units of the system based on an optimal design. The skin-injury monitoring system has a user-friendly interface with a high-speed real-time wireless transmission function. We developed a stable platform firmware and sensible operational software program for the system as well. Furthermore, we fabricated a portable skin-injury monitoring device package via 3D printing. We performed primary experiments in the laboratory using a biological skin-injury model. The developed pressure ulcer sensing system can determine indicators of pressure ulcers and is suitable for the early diagnosis of pressure ulcers and the prevention of skin injury and lesions.

1. Introduction

Decubitus ulcers, also known as pressure ulcers or bedsores, are a skin condition caused by friction, shear, and long-term pressure on the skin. Such ulcers often occur in bedridden individuals who have been confined for a prolonged period owing to paralysis or surgery.[1–3] Macroscopically, direct and indirect factors can cause pressure ulcers. Direct factors such as long-term pressure on the skin can lead to ischemic necrosis,[4–6] whereas indirect factors include skin aging, urinary incontinence, malnutrition, and languishing.

Intense pain due to pressure ulcers causes discomfort to patients, and without prompt treatment, other problems, such as hematomas and open wounds, can occur. In addition, pressure ulcers can lead to complications,[7,8] such as peripheral arterial disease, heart failure, and kidney failure. The development of a pressure ulcer usually comprises four stages, pressure ulcers are difficult to reverse after the first stage, and early diagnosis is important for pain reduction. Thus, techniques for the early detection of pressure ulcers are of research significance. Researchers and engineers have developed early diagnostic techniques and devices for pressure ulcers, which

*Corresponding author: e-mail: chou-ran@aist.go.jp
https://doi.org/10.18494/SAM3601

ISSN 0914-4935
https://myukk.org/

have different advantages and disadvantages. One of the most traditional methods is diascopy.[9] The equipment required is simple and convenient; a small glass plate is used to apply pressure to the skin for a rapid diagnosis. Although this method is widely accepted, it is difficult to obtain a quantitative measure using a glass plate, which results in variation in each diagnosis.[10] Additional disadvantages of diascopy include a lack of recording and remote transmission functions. Ultrasound can also be used to diagnose pressure ulcers with high sensitivity and resolution. However, ultrasound provides similar responses to pressure ulcers and fat; therefore, it may not be suitable for assessments in obese people.[11] In addition, ultrasonic equipment requires considerable space and is expensive; thus, its usage is limited. Subcutaneous moisture meters can be used for the early diagnosis of pressure ulcers,[12] but their operation inevitably affects diagnosis accuracy. Therefore, high-precision and economical test methods for the early diagnosis of pressure ulcers should be developed. Recently, a rapid method has been developed to effectively diagnose pressure ulcers by combining ultraviolet (UV) light with diascopy.[13–15] The effect of different degrees of pressure on the accuracy of measurement in diascopy was studied in detail.[13] The fluctuations in the physical properties of early pressure ulcers and the significance of this UV diascopy method for early detection have also been discussed.[14] However, a portable measuring device combining sensing technology and UV light diascopy has not yet been developed for clinical experiments.

The aim of this study was to develop a portable measuring device for the early detection of pressure ulcers, which would be compact in size and easy to use. By introducing load-cell sensors, the diagnostic pressure can be fed back with high precision. With moderate pressure, blanchable or non-blanchable erythema can be distinguished accurately, and early pressure ulcers can be monitored. White and UV light-emitting diode (LED) arrays were set in the portable device, and their brightness was precisely adjusted to suit different users. To reduce the dependence on medical professionals, we have also identified an artificial-intelligence (AI)-based automatic method that analyzes images to diagnose pressure ulcers. Moreover, the advent of the Internet of Things (IoT) has expanded the application scope of sensing technologies. If a pressure ulcer sensor provides relatively consistent measurements for diagnosis, it will be very useful for research and medical applications in an IoT era.

2. Materials and Methods

2.1 Working principle and device system configuration

For the rapid examination and detection of pressure ulcers, we designed and produced a portable monitoring device. Here, we have introduced the working principle of the device and its configuration. The proposed device works by applying a certain amount of pressure to the patient's skin whilst illuminating the area with UV light.[13,14] The device emits UV light with a wavelength of 405 nm, which can penetrate the surface of the skin. The UV light absorption properties of hemoglobin are then utilized in the dermis to detect the severity of the injury. A simple prototype has been fabricated in a previous study where the UV brightness could be adjusted; however, the prototype lacked features such as pressure feedback, real-time

monitoring, and a camera function.[16] In this study, we have designed a new portable monitoring device, which can quantitatively record the pressure from the diascope, precisely adjust the brightness of UV light and white light, and most importantly observe the patient's skin surface in real time and take high-quality photos for analysis. Figure 1 shows the portable skin-injury monitoring device and the major components within the measurement unit. The monitoring device includes the device package, measurement and platform circuit boards, camera, glass plate, load cell sensors, white and UV LEDs, and batteries. The package and supporting structures of the device were fabricated using a high-accuracy 3D printer (J750 Digital Anatomy, Stratasys Corporation). Figure 1(a) shows the explosion diagram of the designed package structure. A transparent glass plate of 50 × 50 × 5 mm^3 size formed the front panel of the diagnostic system that comes into contact with the skin. A 5-megapixel camera (Imx219pq, SONY Co.) was placed next to the transparent glass plate to capture the probable location of the ulcer for diascopy. At the central line of the glass plate, we placed two loadcell sensors symmetrically, which measured the force by evenly distributing the reaction force of the skin onto the glass plate. Four white LEDs (NFSW757DT-V1, Nichia Corporation) and ten UV LEDs (NCSU275T-U405, Nichia Corporation) were installed on the light source board in the illumination circuit [Fig. 1(b)]. Pressure ulcers usually occur around the patient's buttock or waist. The device is compact enough for users (e.g., nurses, care workers, and doctors) to operate with one hand whilst ensuring that the other hand is available to stabilize the patient lying on their side. The dimensions of the device handle are 80 × 40 × 30 mm^3 [see Fig. 1(c)]. The terminal includes control and record functions [Fig. 1(d)], which are used to adjust the LED intensities, monitor the pressure force, and obtain skin images.

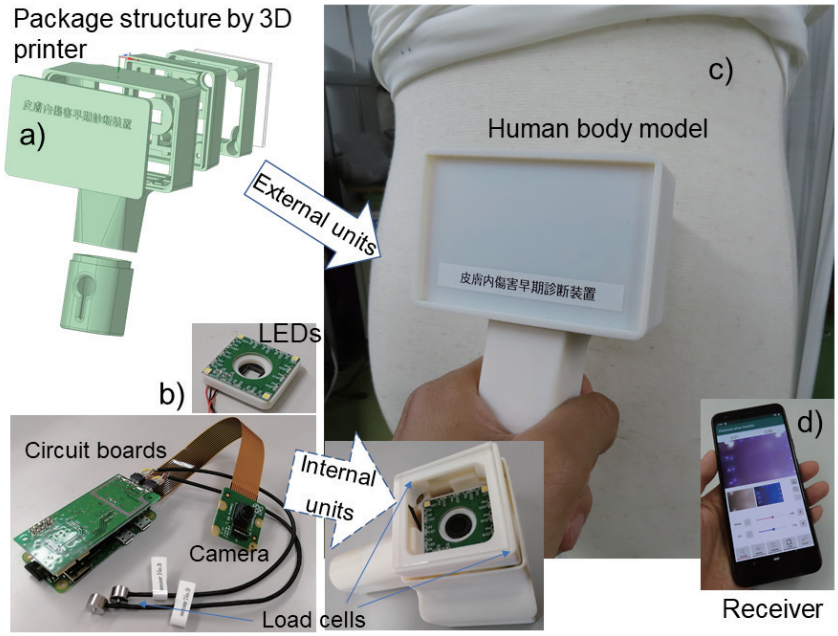

Fig. 1. (Color online) (a) Explosion diagram of portable pressure ulcer monitoring device; (b) inner units including circuit boards, LED arrays, camera, and load cells; and (c) simulated use of device on a human body model. The device is sufficiently compact to be used with one hand. (d) Terminal receiver with control and record functions.

2.2 Operating system firmware configuration

Figure 2 shows a schematic diagram of the operating system for the proposed device. In this study, we designed and manufactured the hardware for the add-on measurement circuit board, completed the firmware, and programmed the software for the platform circuit board. Figure 2(a) shows a diagram of the fabricated measurement circuit board. The circuit board converts a direct current (DC) with the help of a DC converter on the assembled board. The battery voltage was stabilized from 5 V to the required voltages of 4 and 4.5 V. The converted voltages were used to power the load cell and LED driving circuits, respectively. The load cell driving circuit in the measurement board controlled the input and output of the load cells, and the LED driving circuit regulated the luminance from white and UV LEDs. Figure 2(b) shows the schematic of the programmed platform circuit board. A single-board computer (Raspberry Pi Zero, Raspberrypi.org) was used as a platform board. The firmware of the transmission system was developed using this configurable board, and the operating software was programmed. An external high-resolution camera was connected to the platform board to obtain images of pathological changes after programming.

2.3 Animal and pressure ulcer wound models

Eight-week-old healthy male hairless rats (HWY/Slc, SLC Inc.) were used in this study. The rats were fed a standard chow diet and were provided free access to water. They were anesthetized through the intraperitoneal injection of a mixture of anesthetics before the pressure

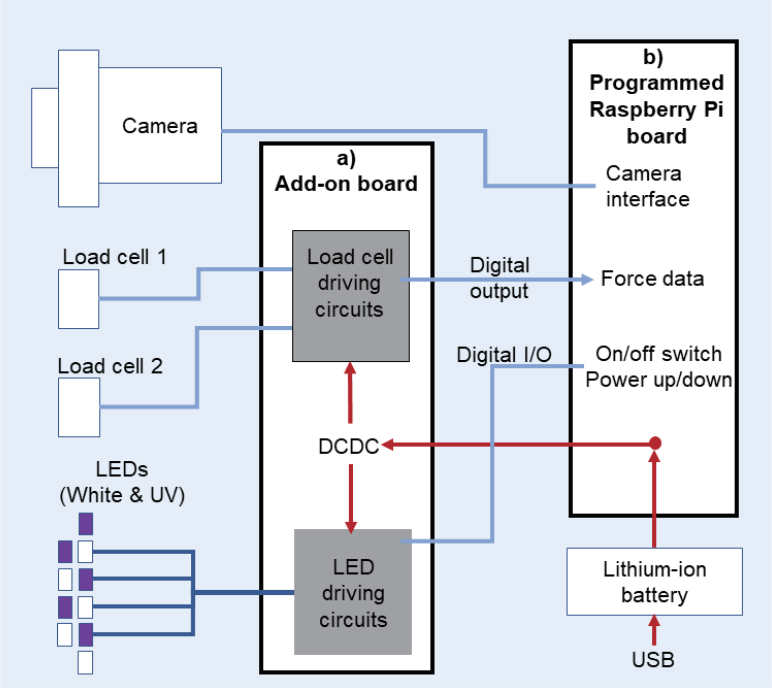

Fig. 2. (Color online) Schematic diagram of firmware.

injure modelling. The pressure injure models were established by pressing the dorsal skin for 4.5 h between two circular neodymium magnets (Niroku Seisakusho Co., Ltd., Japan) with a diameter of 10 mm and a height of 4 mm to exert a stable pressure of 440 mmHg. The relative works were carried out in strict accordance with the Guide for the Care and Use of Laboratory Animals of the National Institutes of Health. The experiments described were conducted with approval (No. 2018-4) from the Animal Experiment Ethics Committee of Nagano College of Nursing.

3. Results

3.1 Device system characteristic evaluation

In preliminary experiments, an average pressure of 8000 Pa was considered for diascopy. The glass plate had a length and width of 50 mm each, and the contact area was determined to be 2500 mm^2. The average measurement force required by this monitoring device was calculated to be 20 N. Figure 3 shows a graph of the output voltage of the load cell (FC8E-50N, Forsentek Corporation) against the load force. We designed and optimized the mechanical structure to ensure a balanced output between the two loadcell sensors. After a reasonable circuit design, fabrication, and calibration, the force and output voltage from the load cell force measuring system appeared to have a linear relationship. The two load cells exhibited a good balanced relationship from 1 to 14 N (see Fig. 3). Therefore, the two load cells that formed the pressure–feedback system could be adjusted between 2 and 28 N for diascopy. These values can meet the initial pressure requirements for the given diagnostic system. Moreover, if a larger or smaller

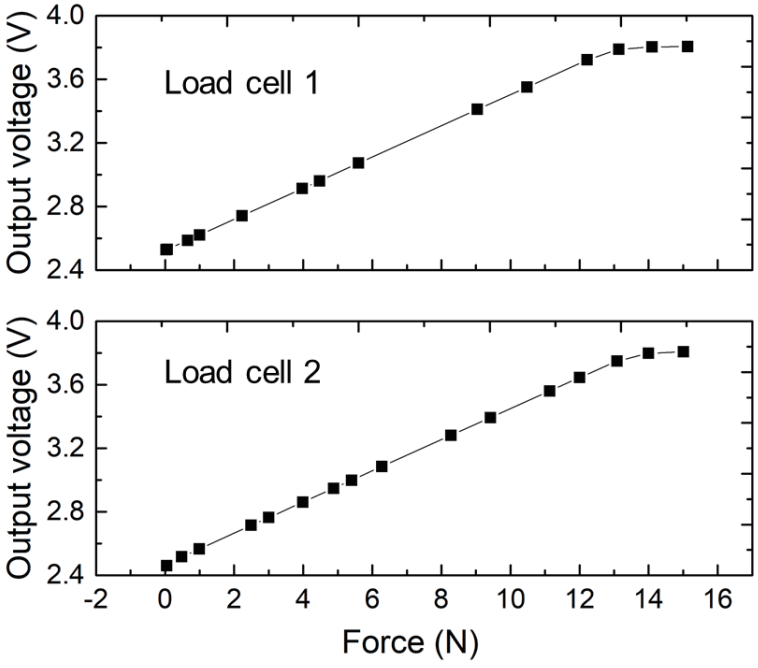

Fig. 3. Calibration of two load cells for pressure control.

pressure range is needed in future empirical experiments, we can appropriately change the contact area of the glass plate, which is also a reasonable method for adjusting the pressure range efficiently.

The LEDs play an important role in this device; the white LEDs illuminate the skin to determine the location of the ulcer, and the UV LEDs diagnose the severity of the pressure ulcer.[15] The patient's skin color will affect the reflectivity of the irradiated light, so the intensities of the two types of LED need to be adjusted accurately. Through the design of the LED control circuit and programming, the proposed device system has a reasonable brightness adjustment function based on hardware and software. Figure 4 shows the results of the calibration of illuminance from the UV and white LEDs. A chroma meter (CL-200A, Konica Minolta Sensing, Inc.) was used to measure the illuminance. The distance between the lighting board and the chroma meter was set to 15 mm, which was the average operating distance between the skin and the LEDs. To ensure the appropriate brightness, the operating system can set 55 brightness stages for each LED, which are between the set values of 75 and 130 for white light and 90 and 145 for UV light. The wide adjustment range for the LED illuminance intensity can fulfill the required intensity variation in the following empirical experiments for different application conditions.

During lighting, the LEDs produce a certain amount of heat. Heat accumulation during prolonged LED usage may damage the equipment and affect the system's stability. Thus, durability towards temperature fluctuations should be implemented to obtain a credible system. For the experiments, the power supply was set at 4 V for the LEDs, and the ambient temperature was 23 °C. Figure 5 shows the surface temperatures of the LEDs during continuous lighting. After 10 min, we observed that the temperature of the white LED rose to approximately 48 °C, whereas that of the UV LED rose to 52 °C. After 80 min, the LED circuit was still working properly, and the surface temperatures of the white and UV LEDs were 65 and 79 °C,

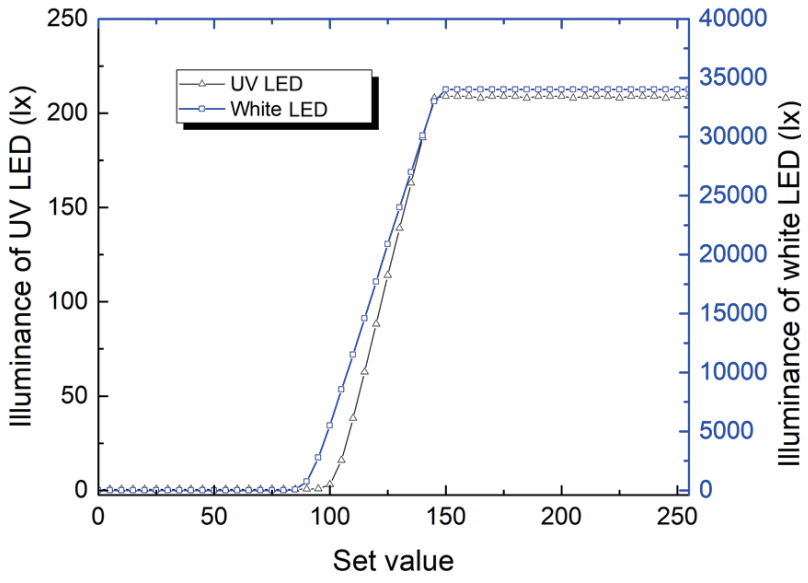

Fig. 4. (Color online) Results of calibration of illuminance from LEDs.

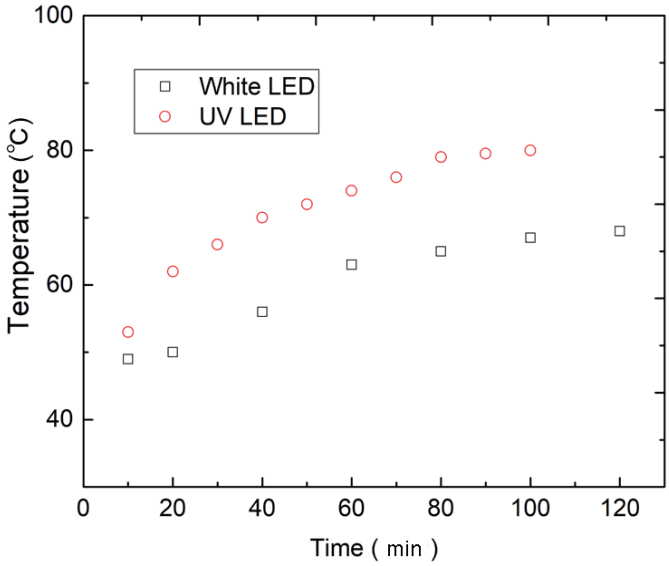

Fig. 5. (Color online) Temperature of LEDs based on continuous lighting time.

respectively. The LED board exhibited a temperature rise; however, there was no risk for the subject because the LEDs were not in direct contact with the subject's skin. Moreover, the technicians usually complete the test and power off the device to cool the LEDs in much less than 10 min; therefore, overheating does not occur.

Power consumption is also an important consideration when developing portable health monitoring devices. Thus, we evaluated the power consumption of the proposed device as well. Figure 6 shows the current flow in the monitor of a device with a wireless transmission function. To evaluate the current flow into the device accurately, we set a 1 Ω shunt resistance (PA-001-0370, NF Corporation) in the power supply circuit. The voltage in the shunt resistance was recorded continuously using an oscilloscope (DLM2024, Yokogawa Corporation). Figures 6(a)–6(d) show the four main working conditions: (a) at 40 s after the device was turned on and the UV and white LEDs had completed the warmup process; (b) a standby mode with minimum power consumption; (c) a working mode with maximum power consumption; and (d) a monitor sleep mode. As shown in Fig. 6, the approximate power consumptions during the warmup, maximum working, and standby modes were 2.5, 3, and 1 W, respectively. A 12 W lithium-ion battery was used to provide power; ideally, the device can operate continuously for 4 h under the maximum working condition and for 12 h during standby.

3.2 Terminal operation interface and preliminary results

3.2.1 Operating software development and a smartphone-based user interface

The control module firmware was programmed using Python (version 3.7.2, www.python.org). A customized android application with a user-friendly interface was developed using the cross-platform programming language, Kotlin (version 1.3.41, www.kotlinlang.org). The

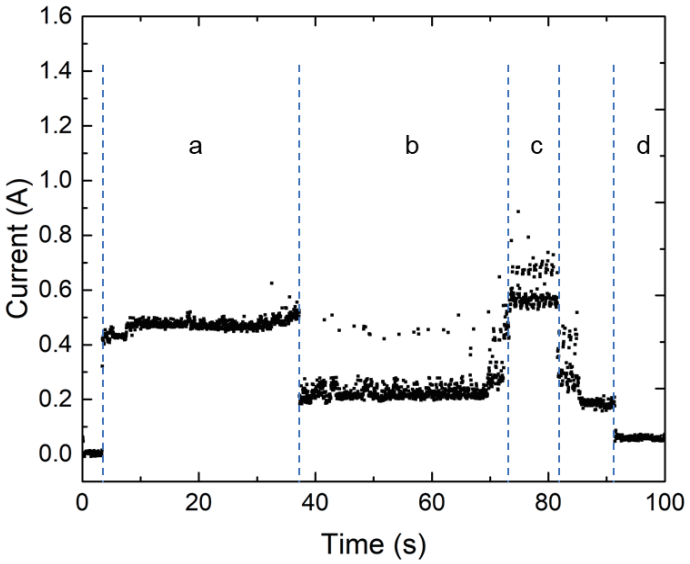

Fig. 6. (Color online) Current flow of the proposed skin-injury monitoring device. The power consumption is obtained from the supply voltage multiplied by the measured current.

application programs, i.e., the pressure ulcer monitoring function and wireless transmission, were developed. Figure 7 shows the user interface of the pressure ulcer diagnostic system; a smartphone (Pixel 4, Google Co.) was used as the terminal operating equipment. The operation page of the monitoring device is shown in Fig. 7(a). The numbers at the top of the operation page indicate the detected force values (0.01 and 0.00) of the load cells. The observation area (middle panel) shows a dynamic image of the area for diagnosis. After the user has selected a potential area of interest, skin surface images under white light and UV light (one each) are acquired and stored in the terminal device. Bars below the real-time monitoring window can be used to adjust the white and UV light intensities for adaptation to different patients. The control icons [Fig. 7(a) bottom] are used to perform other operations, such as image acquisition and real-time monitoring. Figure 7(b) shows the operation system setup page for the pressure ulcer monitoring device. The working threshold of the load-cell sensors, the pixel size of the camera, and the preset brightness range of the LEDs can be adjusted on this page.

3.2.2 Preliminary results obtained using biological pressure injury model

After the device was fabricated, preliminary animal experiments were performed in the laboratory to verify its functionality. Figure 8 shows a comparison between the UV LED and white LED images. Each set consisted of four images of the same area after applying pressure for 12, 24, 36, and 48 h, respectively. We observed that the proposed monitoring device successfully obtained images of the potentially injured area under white and UV light. The acquired images can be analyzed, and pressure ulcers can be diagnosed early. For example, the UV image after 24 h of pressure had darker shading, which is an early indicator of pressure ulcers. This hypothesis was confirmed with LED images after 48 h of pressure, where epidermal

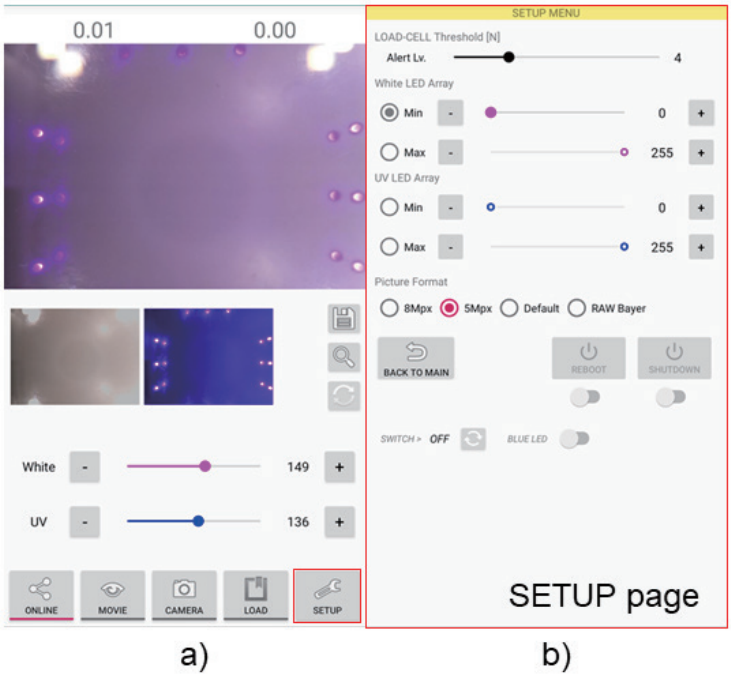

Fig. 7. (Color online) Smartphone-based user interface of the proposed monitoring device. The operation page is shown in (a) and the system setup page is (b).

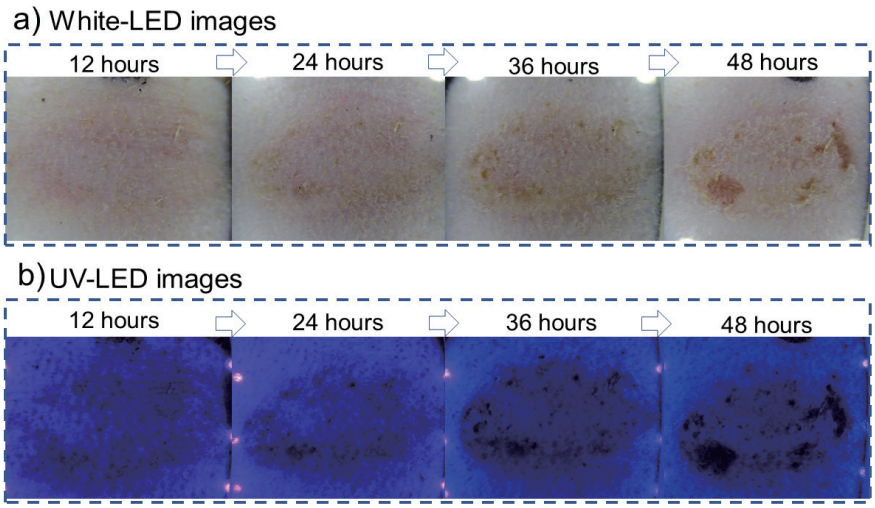

Fig. 8. (Color online) Diagnosis images obtained using white and UV LEDs (12–48 h).

injury was observed. The diagnostic method can be further improved upon with professional analysis and judgment.

Moreover, with improvements in computing speed and cloud technology, the application of AI in rapid medical diagnoses has advanced.[17] Herein, we briefly discuss AI applications in the early diagnosis of pressure ulcers. For the AI-based diagnosis process, image feature extraction

was performed. Initially, pre-processing was performed, and a program was utilized to extract the features of pressure ulcers from original images. Subsequently, using the extracted features, machine learning was performed, and the criteria for the early diagnosis of pressure ulcers were determined. Finally, the diagnosis program for the early detection of pressure ulcers was developed.

As the previous results showed that 24-h UV light images could be used for early pressure ulcer diagnosis, these images were used as a reference to extract characteristic information. Figure 9(a) shows the image of the separated channel (blue, green, and red) histograms from the 24 h UV–LED image. The preliminary results suggest that the blue channel contained information for feature extraction and that the blue-channel image contained more high-contrast shadow information. Thus, all the blue-channel images obtained at 12, 24, 36, and 48 h were extracted for comparison [see Figure 9(b)]. The blue channel image was subjected to the next step of contour detection analysis, and the shadow area and outline were specified. The shadow area and outline pattern can be used as the basis for the early diagnosis of pressure ulcers [see Fig. 9(c)]. In future work, we would like to develop more advanced algorithms to predict pressure ulcers, e.g., coding a program that can automatically reveal the degree of relationship between the shadow area outline and the presence and severity of pressure ulcers, and we hope to present this analysis in our subsequent studies.

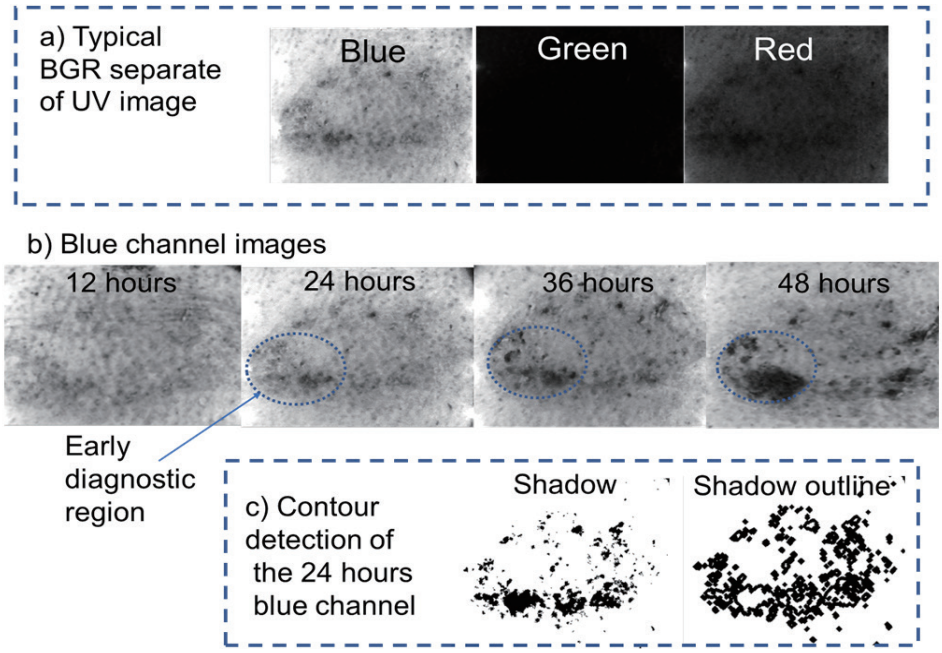

Fig. 9. (Color online) Preliminary analysis results obtained using portable pressure ulcer monitoring device in a laboratory setup. (a) Typical images of the separated channel (blue, green, and red) histograms of the skin image. (b) Blue-channel images of the skin at 12–48 h. (c) Shadow area and shadow outline specified from the blue separated channel.

4. Conclusions and Outlook

In this study, we developed a portable skin-injury monitoring device for the early diagnosis of pressure ulcers. We also developed the platform firmware and programmed the software for a real-time monitoring system with a user-friendly interface and a high-speed wireless transmission system. By leveraging 3D printing techniques, a portable skin-injury monitoring device was successfully manufactured. Preliminary measurements were performed in the laboratory, and the device determined indicators for the early diagnosis of pressure ulcers, such that the deterioration of the condition can be prevented.

Although the monitoring methods in the clinic are important for the early diagnosis of pressure ulcers, the configuration of this device needs to be adjusted further to ensure compatibility, and the size and power of sensors should be optimized. Additional efforts are required to evaluate the sensor system in a clinical setting with the involvement of healthcare professionals. Moreover, the assistance software of automatic diagnosis and analysis based on AI should also be well developed to improve the accuracy and efficiency of field diagnosis and reduce the burden on nurses and doctors.

Acknowledgments

This work was partly supported by JSPS KAKENHI (Grant number: 21H03269).

References

1 L. Schoonhoven, T. Defloor, and M. H. F. Grypdonck: J. Clin. Nurs. **11** (2002) 779. https://doi.org/10.1046/j.1365-2702.2002.00621.x.
2 J. Webster, C. Lister, J. Corry, M. Holland, K. Coleman, and L. Marquart: J. Wound Ostomy Continence Nurs. **42** (2015) 138. https://doi.org/10.1097/WON.0000000000000092
3 F. Aloweni, S. Ang, S. Fook-Chong, N. Agus, P. Yong, M. Goh, L. Tucker-Kellogg, and R. Soh: Int. Wound J. **16** (2019) 164. https://doi.org/10.1111/iwj.13007
4 C. Dealey: Adv. Skin Wound Care **22** (2009) 421. https://doi.org/10.1097/01.ASW.0000360255.92357.ad.
5 K. Bernabe: Curr. Opin. Pediatr. **24** (2012) 352. https://doi.org/10.1097/MOP.0b013e32835334a0
6 J. Mervis and T. Phillips: J. Am. Acad. Dermatol. **81** (2019) 881. https://doi.org/10.1016/j.jaad.2018.12.069
7 E. Jaul: Assessment and Management of Pressure Ulcers in the Elderly: Drugs Aging **27** (2010) 311. https://doi.org/10.2165/11318340-000000000-00000
8 F. Xiao, H. Peng, and Y. Li: Am. J. Transl. Res. **13** (2021) 3515. https://www.ncbi.nlm.nih.gov/pmc/articles/PMC8129310
9 Institution of diascopy diagnosis: https://knowledge.nurse-senka.jp/1087/ (accessed June 2021).
10 S. Sprigle, M. Linden, and B. Riordan: Ostomy Wound Manag. **49** (2003) 42. https://pubmed.ncbi.nlm.nih.gov/12732750/
11 E. Andersen and T. Karlsmark: Skin Res. Technol. **14** (2008) 270. https://doi.org/10.1111/j.1600-0846.2008.00290.x
12 A. Budri, Z. Moore, D. Patton, T. O'Connor, L. Nugent, and P. Avsar: Int. Wound J. **17** (2020) 1615. https://doi.org/10.1111/iwj.13437
13 E. Takashi, Y. Wang, D. Miura, P. Hou, H. Xue, and A. Kitayama: 2019 National Pressure Ulcer Advisory Panel Annual Conf. (NPUAP, St. Louis, USA 2019).
14 E. Takashi, Y. Wang, H. Xu, D. Miura, and A. Kitayama: 2020 National Pressure Ulcer Advisory Panel Annual Conf. (NPUAP, Houston, USA, 2020).

15 Y. Wang, H. Xu, A. Kamijo, K. Kondou, A. Kitayama, and E. Takashi: Jpn. J.P.U. **23** (2021) 326.
16 H. Xu, Y. Wang, E. Takashi, A. Kamijo, D. Miura, K. Karasawa, A. Kitayama, J. Lu, and L. Zhang: Int. Wound J. **19** (2022) 834. https://doi.org/10.1111/iwj.13681
17 T. Yasuda, T. Hiroyasu, S. Hiwa, Y. Okada, S. Hayashi, Y. Nakahata, Y. Yasuda, T. Omatsu, A. Obora, T. Kojima, H. Ichikawa, and N. Yagi: Dig. Endosc. **32** (2020) 373. https://doi.org/10.1111/den.13509